Study of Traps in Special Doped Optical Fiber Radiation Sensors via Glow Curve Analysis

Mostafa Ghomeishi[1,4]*, G Amouzad Mahdiraji[1], Peyman Jahanshahi[1], FR Mahamd Adikan[1] and David A Bradley[2,3]

[1]Integrated Lightwave Research Group, Faculty of Engineering, University of Malaya, 50603Kuala Lumpur, Malaysia
[2]Department of Physics, University of Malaya, 50603 Kuala Lumpur, Malaysia
[3]Department of Physics, University of Surrey, Guildford, GU2 7XH, UK
[4]Faculty of Science, Science and Research branch, Islamic Azad University, Tehran, 14778, Iran

Abstract

Thermoluminescence dosimeters (TLDs) are widely used, serving the needs of various radiation applications. In recent times optical fibers have been introduced as alternatives to more conventional phosphor-based TLD systems, with many efforts being carried out to improve their thermoluminescence (TL) yield. While there have been extensive studies of many of the various TLD characteristics of optical fibers, including TL response, linearity, reproducibility, repeatability, sensitivity and fading, far more limited studies have concerned dependence on the type of TL activator used in optical fibers, promoting the TL mechanism. Present study focuses on TLD glow curves analysis for five different doped optical fibers that have been subjected to photon and electron irradiation. Trap parameters such as activation energy and frequency factors have been obtained from second order kinetics analysis, based on computerized glow curve deconvolution. An interesting observation is that co-doped fibers typically leads to enhanced TL characteristics, pointing to a need for optimization of the choice and levels in use of co-dopants.

Introduction

New perspectives are evolving in respect of the wide range of potential thermoluminescence dosimetry (TLD) applications of various forms of optical fiber [1,2]. As an instance, optical fiber TLDs has been shown to be effective for a range of photon sources, from visible and UV, through to x- and gamma-rays of different energies [3-5]. Further studies have concerned silica fibers of various shape and doped-core dimension, flat optical fibers being shown to lead to improved TL response [6-10], it also being demonstrated that the TL response of fibers will vary depending upon core dopant concentration as well as core size [11-13].

Although commercial TLDs have typically developed, following up upon the favourable outcome of studies of various constituents, for optical fibers the study of TL yield have been much more limited, most typically with germanium, aluminum, oxygen, phosphorus and nanomaterial cluster dopants [4,14-16]. Present study seeks to help address this lack, expanding investigations to include additional rare-earth dopants, examining TL response and associated kinetics analysis of such optical fibers.
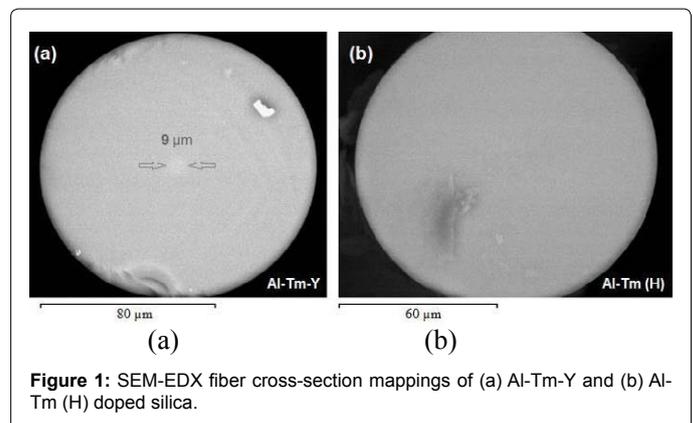
The characterization of the defect centers forms a crucial step in understanding the mechanism of TL [17]. In this context, analysis of glow curves offers a sensitive and suitable technique for such study. Here, in present study, new materials are tested to examine their effect, both on TL response and kinetic parameters.

Method and Materials

Optical fiber fabrication and preparation

The samples are standard circular cross-section optical fiber of 125 μm outer diameter, fabricated using the facilities of the University of Malaya fiber pulling lab. The 9 μm central core that forms the dopant channel has been confirmed using the energy-dispersive x-ray (EDX) facility of an SEM, doped-core and silica cladding mappings being obtained for all but one of the samples (Figure 1). For Al-doped fiber,

EDX mapping of the core represents a severe challenge, due to the neighbouring atomic numbers of Al (Z=13) and Si (Z=14), providing for limited differential X-ray fluorescence production, further confounded by the associated low energy emissions (Figure 1b). The doped elements are compared with SiO_2, BaF, GaP, Al_2O_3, TmF_3 as a reference for EDX identification. The characteristic peaks through which the dopant materials are detected are $K_{\alpha 1}$ for O, Si, Al, Y, Ba and Ga and $L_{\alpha, \beta}$ for Tm. Table 1 shows the concentration of each element present in the different samples.

Figure 1: SEM-EDX fiber cross-section mappings of (a) Al-Tm-Y and (b) Al-Tm (H) doped silica.

Element	Al-Y-Tm	Ba	Al-Tm (H)	Al-Tm (L)	Ga
O	52.66	51.13	54.52	55.09	52.79
Si	46.42	43.27	40.11	41.02	41.81
Ba	-	5.6	-	-	-
Ga	-	-	-	-	5.4
Tm	0.25	-	0.24	0.18	-
Al	0.54	-	5.13	3.71	-
Y	0.13	-	-	-	-

Table 1: EDX results for the different doped fiber samples. In this table the weight percentage of each material is shown.

The outer polymer cover to the fibers has been carefully removed using a chloroform solution, soaking the fibers in the solution for 30 seconds. The samples are subsequently cleaned with acetone and carefully cut to 5 mm lengths using a fiber cleaver. Two sets of five samples each were chosen from each type of fiber, the uncertainty in fiber length being ± 0.5 mm. Since the fiber samples have closely identical mass density, also being carefully selected for uniform length, mass normalization of the results has not been required in carrying out analysis and comparisons.

Irradiation and readout

Prior to any irradiation run, in order to remove any prior radiation history, all samples are annealed at 400°C for one hour, subsequently cooled to room temperature. The samples have then been exposed to a dose of 8 Gy dose delivered either by 6 MeV electrons or 6 MV photons, use being made of a Varian 2100 C linear accelerator. The samples were positioned on the surface of a *solid-water^{TM}* phantom. The field size and surface to source distance were set at 20×20 cm^2 and 100 cm respectively. A square applicator with 20×20 cm^2 aperture size was used for electron irradiation.

The TL response of radiated samples was obtained using a Harshaw 3500 TLD reader, the irradiated samples being thermally stimulated from 50°C to 400°C, provided at a heating rate of 20°C/s. The generated glow curves have been analyzed using a second order kinetics model for TL deconvolution.

Results and Discussion

The differential TL responses of the five sets of optical fibers with respect to a dose of 8 Gy are illustrated in Figure 2 for both photon and electron irradiations. The TL yields are similar for both the photon and electron irradiations, with a deviation between them of less than 4% based on the mean values.

In Figures 3-7 the main glow curves for each of the fiber samples have been deconvoluted, with a figure of merit (FOM) for fitting of about 3.4-5.2% and a mean deviation of 0.8%. The extracted traps information from the deconvolution of glow curves is presented in Tables 2-6. In the tables, E_a is the activation energy of each trap in units of eV, s' is the first derivative of the frequency factor (s^{-2}), n_0 is the initial concentration of trapped electrons (cm^{-3}). The Peak-I and Peak-T values are the glow curves maximum intensity (μC) and associated relevant temperature (°C) respectively. The full-width-half-maximum (FWHM) value is calculated on the absolute temperature scale and the TL emission wavelength is in units of nm.

Tables 2-6 show the first peak (referred to as Trap 1) to have an activation energy of 0.9-1.1 eV, a peak intensity of 2-2.9 μC, and an emission wavelength of between 1100 and 1400 nm pointing to independence from the dopant material, instead being more related to

the substrate or the silica preform itself. The activation energy suggests association between O_2 and O^{2-} defects in amorphous and fused silica [18].

Examining Figures 2-4, the numerous traps in Al-Y-Tm-doped and Ba-doped fiber provide for the greater response of these two forms over that of other samples, each of which are composed of lesser numbers of traps (Figures 5-7). This supports the underpinning basis of greater numbers of traps producing greater absorption. According to Figure 3 the combination of Al, Y and Tm as fiber co-dopants results in an increased number of trap centres and, as a result, enhanced absorption. Figure 4 for Ba-doped silica, provides for lower intensity glow peaks compared to that for Al-Y-Tm-doped fiber, albeit with similar energy traps formed in the two types of fiber.

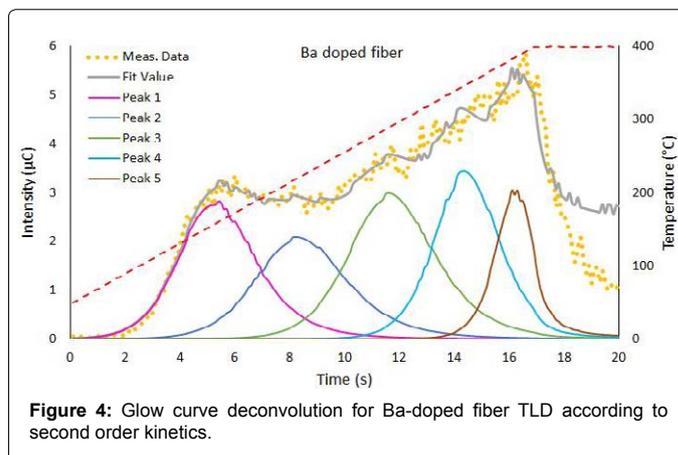In accord with Tables 2 and 3, the major difference between Al-Y-Tm-doped fiber and Ba-doped fiber is the intensity of the individual
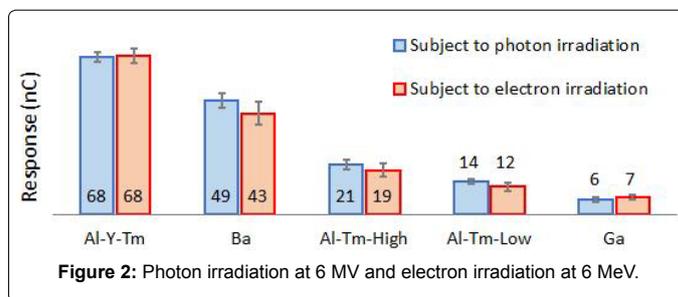

Figure 2: Photon irradiation at 6 MV and electron irradiation at 6 MeV.
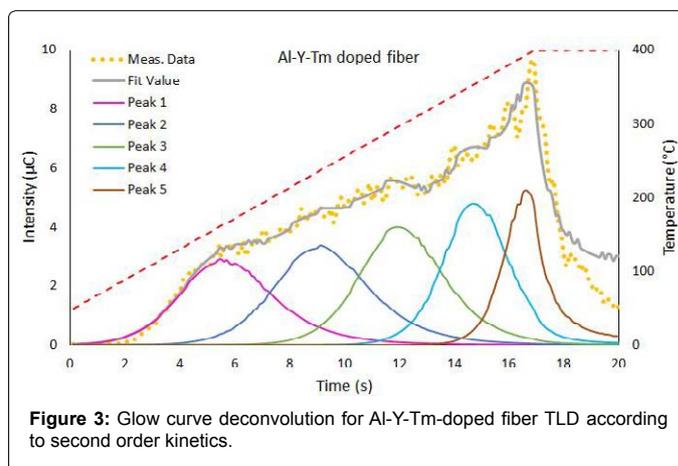
Figure 3: Glow curve deconvolution for Al-Y-Tm-doped fiber TLD according to second order kinetics.

Figure 4: Glow curve deconvolution for Ba-doped fiber TLD according to second order kinetics.

Figure 5: Glow curve deconvolution for high concentration Al-Tm-doped fiber TLD according to second order kinetics.

Figure 6: Glow curve deconvolution for low concentration Al-Tm-doped fiber TLD according to second order kinetics.

Figure 7: Glow curve deconvolution for Ga-doped fiber TLD according to second order kinetics.
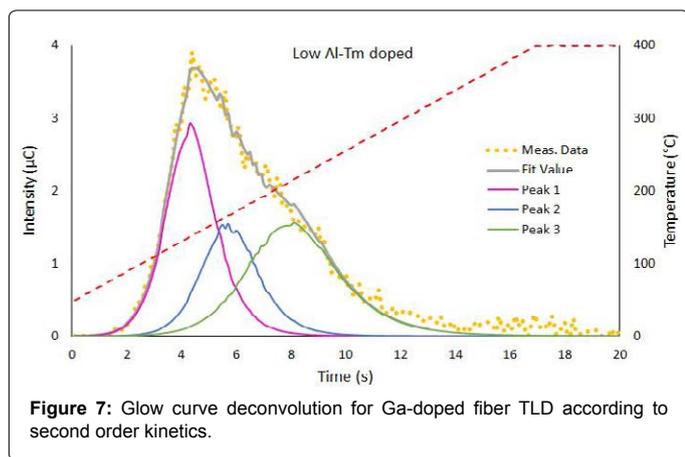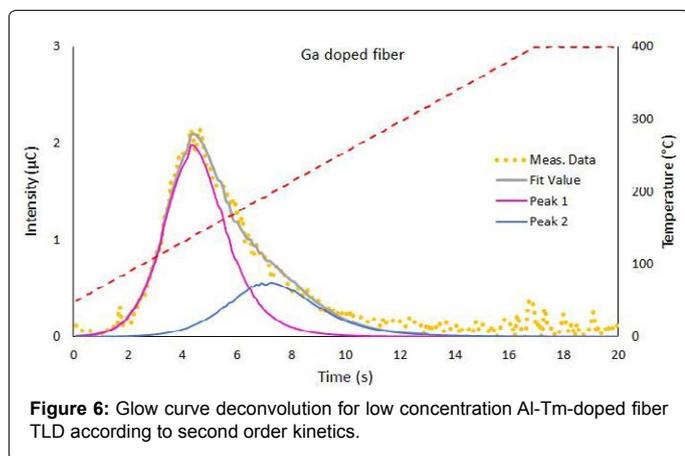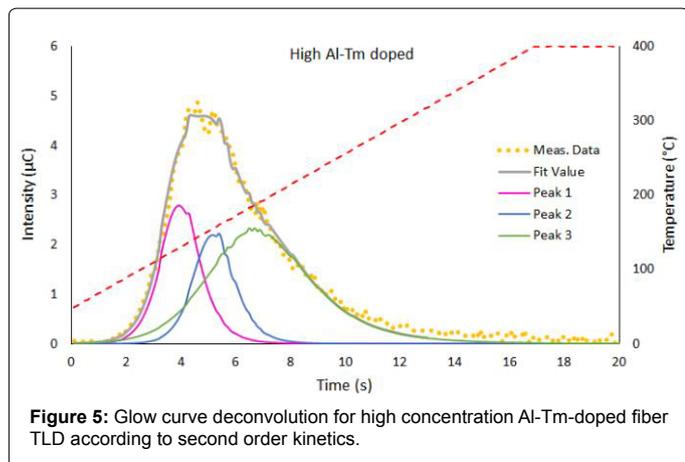
peaks. In the first case, the more energetic traps have the greater capacity for storing memory of the irradiation. The complex shape of the Ba-doped fiber glow curve is posited to be due to deep interactions of this element with the host silica preform.

Figures 5 and 6 show deconvolutions for optical fibers containing the same dopant (Al-Tm), one with a greater concentration of Al inside the fiber core than the other. Tables 4 and 5 show that in increasing this dopant concentration, there is no practical change in the peak positions (peak $T \approx 160\text{-}166$ and $193\text{-}206$ for traps 2 and 3 respectively), but the intensity is increased, the exception being for trap 1 which is

independent of dopant as discussed earlier (peak I_1=1.5 and 1.6 → peak I_2=2.2 & 2.3 for traps 2 and 3 respectively).

The simple glow curve of Ga-doped fiber is shown in Figure 7. The

Al-Y-Tm doped					
	Trap: 1	**Trap: 2**	**Trap: 3**	**Trap: 4**	**Trap: 5**
E_a	1.1	0.9	1.2	2.0	3.0
s'	1.3e3	1.6e4	5.7e6	5.3e11	9.0e19
n_0	1.4e4	1.6e4	1.6e4	1.5e4	4.1e3
Peak I	2.9	3.4	4.0	4.8	5.2
Peak T	162	237	295	353	393
FWHM	79	81	73	54	29
Emission	1138	1438	993	628	408

Table 2: Trap parameters for Al-Y-Tm-doped fiber.

Ba doped fiber					
	Trap: 1	**Trap: 2**	**Trap: 3**	**Trap: 4**	**Trap: 5**
E_a	1.0	0.8	1.2	1.9	3.0
s'	6.7e4	3.7e4	2.3e6	4.7e11	1.5e21
n_0	1.1e4	9.2e3	1.2e4	1.1e4	1.0e3
Peak I	2.8	2.1	3.0	3.4	3.1
Peak T	166	241	297	345	403
FWHM	65	79	73	54	31
Emission	1238	1463	1055	644	408

Table 3: Trap parameters for Ba-doped fiber.

High Al-Tm doped			
	Trap: 1	**Trap: 2**	**Trap: 3**
E_a	1.1	1.5	0.6
s'	1.9e13	1.6e14	7.2e2
n_0	5.8e3	4.5e3	1.1e4
Peak I	2.8	2.2	2.3
Peak T	128	160	193
FWHM	33	33	86
Emission	1145	829	1916

Table 4: Trap parameters for high concentration of Al-Tm-doped fiber.

Low Al-Tm doped			
	Trap: 1	**Trap: 2**	**Trap: 3**
E_a	1.1	1.1	0.8
s'	7.6e9	2.0e9	4.3e4
n_0	6.8e3	4.3e3	6.7e3
Peak I	2.9	1.5	1.6
Peak T	137	166	206
FWHM	42	48	77
Emission	1128	1111	1503

Table 5: Trap parameters for low concentration of Al-Tm-doped fiber.

Ga doped fiber		
	Trap: 1	**Trap: 2**
E_a	0.9	0.8
s'	1.3e7	6.9e4
n_0	6.0e3	2.4e3
Peak I	2.0	0.6
Peak T	139	197
FWHM	50	77
Emission	1398	1600

Table 6: Trap parameters for Ga-doped fiber.

main TL is generated from the first glow peak which is from the silica preform, while lesser TL is contributed from peak 2, from Ga traps.

Conclusion

The similarity in activation energy of first glow peak for all fiber samples indicates the TL response of the substrate, regardless of the dopant in the fiber. It is concluded that different concentration of similar dopant will only affect the intensity of relevant glow peaks while other factors will remain the same. An interesting observation from this study is that co-doping of the fiber is associated with an increase in the TL yield, pointing to a need for optimization of the choice and levels in use of co-dopants.

References

1. Yusoff AL, Hugtenburg RP, Bradley DA (2005) Review of development of a silica-based thermoluminescence dosimeter. Radiation Physics and Chemistry 74: 459-481.

2. Bradley DA, Hugtenburg RP, Nisbet A, Abdul Rahman AT, Issa F, et al. (2012) Review of doped silica glass optical fibre: their TL properties and potential applications in radiation therapy dosimetry. Appl Radiat Isot, 71: 2-11.

3. Abdul Rahman T, Abu Bakar NK, Chandra Paul M, Bradley DA (2014) Ultraviolet radiation (UVR) dosimetry system and the use of Ge-doped silica optical fibres. Radiation Physics and Chemistry.

4. Girard S, Ouerdane Y, Marcandella C, Boukenter A, Quenard S, et al. (2011) Feasibility of radiation dosimetry with phosphorus-doped optical fibers in the ultraviolet and visible domain. Journal of Non-Crystalline Solids 357: 1871-1874.

5. Issa F, Latip NAA, Bradley DA, Nisbet A (2011) Ge-doped optical fibres as thermoluminescence dosimeters for kilovoltage X-ray therapy irradiation. Nuclear Instruments and Methods in Physics Research Section A: Accelerators, Spectrometers, Detectors and Associated Equipment 652: 834-837.

6. Bradley DA, Abdul Sani SF, Alalawi AI, Jafari SM, Noor M, et al. (2014) Development of tailor-made silica fibres for TL dosimetry. Radiation Physics and Chemistry 104: 3-9.

7. Bauk AS, Abdul-Rashid HA, Gieszczyk W, Hashim, Mahdiraji GA, et al. (2014) Potential application of pure silica optical flat fibers for radiation therapy dosimetry. Radiation Physics and Chemistry 106: 73-76.

8. Ghomeishi M, Mahdiraji GA, Adikan FM, Ung N, Bradley (2015) Sensitive Fibre-Based Thermoluminescence Detectors for High Resolution In-Vivo Dosimetry. Scientific reports 5.

9. Amouzad Mahdiraji G, Ghomeishi M, Dermosesian E, Hashim S, Ung NM, et al. (2015) Optical fiber based dosimeter sensor: beyond TLD-100 limits. Sensors and Actuators A: Physical 222: 48-57.

10. Ghomeishi M, Mahdiraji GA, Adikan FRM, Hashim S (2013) The thermoluminescence response of undoped silica PCF for dosimetry application. In: Lasers and Electro-Optics Pacific Rim (CLEO-PR), 2013 Conference: 1-2.

11. Zahaimi NA, Ooi Abdullah MHR, Zin H, Abdul Rahman AL, Hashim S, et al. (2014) Dopant concentration and thermoluminescence (TL) properties of tailor-made Ge-doped SiO_2 fibres. Radiation Physics and Chemistry.

12. Ghomeishi M, Jahanshahi P, Dermosesian E, Adikan FR (2014) Analysis of optical fibre defects using thermoluminescence glow curve method. In: Photonics (ICP), 2014 IEEE 5th International Conference: 141-143.

13. Bradley DA, Mahdiraji G, Ghomeishi M, Dermosesian E, Adikan, et al. (2014) Enhancing the radiation dose detection sensitivity of optical fibres. Applied Radiation and Isotopes 100: 43-49.

14. Abdulla YA, Amin Y, Bradley DA (2001) The thermoluminescence response of Ge-doped optical fibre subjected to photon irradiation. Radiation Physics and Chemistry 61: 409-410.

15. Wagiran H, Hossain I, Bradley D, Yaakob ANH, Ramli (2012) Thermoluminescence Responses of Photon and Electron Irradiated Ge- and Al-Doped SiO_2 Optical Fibres. Chinese Physics Letters 29: 027802.

16. Salah N (2011) Nanocrystalline materials for the dosimetry of heavy charged particles: A review. Radiation Physics and Chemistry 80: 1-10.

17. Rasheedy MS (2005) A modification of the kinetic equations used for describing the thermoluminescence phenomenon. J Fluoresc 15: 485-491.

18. Salh R (2011) Defect related luminescence in silicon dioxide network: a review. In: Crystalline Silicon - Properties and Uses 135-172.